Applying models of pulsar wind nebulae to explain X-ray plateaux following short Gamma-Ray Bursts

L. C. Strang* and A. Melatos

School of Physics, University of Melbourne,
Parkville, VIC 3010, Australia
** E-mail: lstrang@student.unimelb.edu.au*

Australian Research Council Centre of Excellence in Gravitational-wave Discovery (OzGrav),
School of Physics, University of Melbourne,
Parkville, VIC 3010, Australia
** E-mail: lstrang@student.unimelb.edu.au*

Many short Gamma-Ray Bursts (sGRBs) have a prolonged plateau in the X-ray afterglow lasting up to tens of thousands of seconds. A central engine injecting energy into the remnant may fuel the plateau. A simple analytic model describing the interaction of the magnetized relativistic wind from a rapidly-rotating magnetar with the surrounding environment can reproduce X-ray plateaux and instantaneous spectra. The model is analogous to classic, well-established models of young supernova remnants and applies the underlying physics to sGRB remnants. The light curve and spectra produced by the model are compared to observations of GRB 130603B. The spectra are also used to estimate parameters of the magnetar including its poloidal field strength and angular frequency. If combined with a gravitational wave signal, this model could provide insight into multimessenger astronomy and neutron star physics.

Keywords: Gamma-ray bursts; afterglow; supernova remnants

1. Introduction

Many short gamma-ray bursts (sGRBs) display long-lived emission in the X-ray band. A subset of the X-ray afterglows are "canonical" afterglows with three components: an initial decay, a flat plateau lasting from 10 s – 10^5 s, and a final decay (typically $\sim t^{-2}$).[1,2] The luminosity and duration of the plateau are correlated, with brighter plateaux ending sooner.[3] A similar phenomenon is observed in long gamma-ray bursts (LGRBs), but the two populations are statistically distinct and likely have different progenitors for the afterglow as well as the prompt emission.[4–6]

Binary neutron star coalescence has been confirmed as a progenitor of sGRBs,[7,8] suggesting the evolution of the post-merger remnant dictates the evolution of the afterglow. X-ray plateaux have inspired several models including fireballs (with[9,10] and without[11] energy injection), fall-back accretion onto a black hole,[12] and ongoing energy injection via a central engine,[13] commonly assumed to be a millisecond magnetar.[14] In the latter scenario, the rotational energy of the magnetar is converted to X-rays via an unknown dissipative process, perhaps involving a relativistic wind.[13–19] Previous models have considered the evolution of a magnetar surrounded

by a shroud of optically-thick ejecta material[20–22] or the production of X-rays via radiative losses from interactions with the surrounding environment.[23,24]

In this work, we present results from Ref. 25 and Ref. 26 exploring a millisecond magnetar central engine through the lens of classic models of pulsar wind nebulae (PWNe), also known as plerions. The term plerion is used throughout Ref. 25 and Ref. 26. Here, we use the term PWNe throughout to emphasize the analogy to supernova remnant models such as Ref. 27 (although technically, we are discussing a magnetar wind nebula and not a pulsar wind nebula). In the PWNe model, the X-ray plateau is caused by a magnetized bubble of electrons fuelled by the relativistic wind of the magnetar. We summarize the model presented in Ref. 25 in Sec. 2 and explore associated synchrotron light curves in Sec. 3. In Sec. 4, we quote results from Ref. 26 inferring parameters of the central engine using instantaneous spectra. We conclude in Sec. 5. This paper borrows substantially from the form and content of Ref. 25 and Ref. 26; among other things, it includes Fig. 3 from Ref. 26 unchanged.

2. Pulsar Wind Model

If a neutron star survives the sGRB, it evolves under the same physics that dictates the early evolution of PWNe. Classic one-zone models for PWNe provide an analytic estimate of the synchrotron luminosity of the remnant without specifying its detailed geometry.[27,28] In Ref. 25, an analogous model is developed and applied to X-ray plateaux. In this scenario, the sGRB heralds the birth of a rapidly-rotating neutron star with a dipole, magnetar-strength external magnetic field with angular frequency $\Omega(t)$, initial angular frequency Ω_0, and polar surface magnetic field strength B_0. Simultaneously, an isotropic, relativistic blast wave (described by the Blandford-McKee self-similar solution[29]) detonates and sweeps up the surrounding interstellar medium into a spherical shell expanding at $v_{\rm s}$.

The neutron star spins down under pure magnetic-dipole braking and radiates energy at a rate

$$L_{\rm sd}(t) = L_0 \left(1 + \frac{t}{\tau}\right)^{-2} \tag{1}$$

where $L_0 \propto B_0^2 \Omega_0^4$ is the initial spin-down luminosity and $\tau \propto B_0^{-2} \Omega_0^{-2}$ is the characteristic spin-down timescale. Through analogy with classic models of PWNe, we assume the energy is extracted as a magnetized, relativistic electron-positron wind with velocity $v_{\rm w} \gg v_{\rm s}$. The ratio of the Poynting flux to kinetic-energy flux in the wind, σ, is expected to be $\gtrsim 1$ (i.e. the wind is Poynting-flux dominated) near the star and $\ll 1$ (i.e. kinetic-energy flux dominated) at distances far beyond the co-rotation radius $c/\Omega(t)$ ($\sigma \approx 10^{-3}$ for the Crab[30–32]).

As in PWNe, a reverse shock forms at radius $r_{\rm rs}$ where the ram pressure of the wind $P_{\rm ram}(r)$ balances the external static pressure $P_{\rm stat}(r)$.[28] As the shock propagates into the wind, the electrons are shocked into a power-law energy distribution $\propto E^{-a}$. Reference 25 models the electron population with a spherical, homogeneous

bubble characterized by its properties at $r_{\rm rs}$ (i.e. at $r = \dot{r}_{\rm rs}t$ for constant $\dot{r}_{\rm rs}$). Under this assumption, the fresh electrons in the energy range $[E_{-0}, E_{+0}]$ are injected into the bubble at a rate

$$\dot{N}_{\rm inj} = \frac{L_{\rm sd}(t)E^{-a}(a-2)}{(1+\sigma)\left(E_{-0}^{2-a} - E_{+0}^{2-a}\right)}. \tag{2}$$

The bubble expands at a rate $\dot{r}_{\rm rs}$, so electrons cool according to adiabatic expansion at a rate

$$-\left.\frac{{\rm d}E}{{\rm d}t}\right|_{\rm adiabatic} = \frac{E}{t}. \tag{3}$$

Given a magnetic field in the bubble $B(t)$, the electrons also cool via synchrotron radiation at a rate

$$-\left.\frac{{\rm d}E}{{\rm d}t}\right|_{\rm synch} = c_s E^2 B(t)^2 \tag{4}$$

where $c_s = \mu_0 e^4/9\pi c^3 m_e^4$. Two magnetic field configurations are presented in Ref. 25. In the first case, henceforth model A, $B(t)$ is taken to be the far-field extension of the stellar dipole field at radial distance $\dot{r}_{\rm rs}t$ (see Eq. (9) in Ref. 25). In the second case, henceforth model B, $B(t)$ is taken to be an arbitrary, constant B. Model B serves two purposes. One, it allows the PWNe model (including magnetar spin down, electron injection, and cooling mechanisms) to be assessed in general terms, even if the specific magnetic field structure in model A is a poor approximation to reality. Two, model B decouples $B(t)$ and the central engine parameters B_0 and Ω_0 (which also govern $\dot{N}_{\rm inj}$), allowing for the possibility that $B(t)$ may be affected by components of the post-merger environment other than the central engine.

The number density of electrons per unit energy $N(E,t)$ can be found via the time-dependent, inhomogeneous partial-differential equation

$$\frac{\partial N(E,t)}{\partial t} = \frac{\partial}{\partial E}\left[\left.\frac{{\rm d}E}{{\rm d}t}\right|_{\rm adiabatic} + \left.\frac{{\rm d}E}{{\rm d}t}\right|_{\rm synch}\right] + \dot{N}_{\rm inj} \tag{5}$$

where adiabatic cooling is defined as in Eq. (3), synchrotron cooling is defined in Eq. (4), and electron injection $\dot{N}_{\rm inj}$ is defined in Eq. (2). Two analytic Green's function solutions (corresponding to models A and B) are found in Ref. 25 and integrated to obtain $N(E,t)$.

3. Light Curves

In this section, we highlight results from Ref. 25 comparing the X-ray synchrotron light curves predicted by the model in Sec. 2 to those observed by the Neil Gehrels *Swift* telescope.[33–35]

The synchrotron spectrum of an electron with energy $E_{\rm c}$ may be approximated as a Dirac-delta function centred at the characteristic synchrotron frequency

$\nu_c \propto E_c^2 B(t)$. The source frame synchrotron luminosity in the range $[\nu_{\rm min}, \nu_{\rm max}]$ is

$$L_{\nu_{\rm min}-\nu_{\rm max}} = \int_{\nu_{\rm min}}^{\nu_{\rm max}} {\rm d}\nu c_s B(t)^2 E_c^2 N(E_c, t). \quad (6)$$

We define $L_{\rm X}$ as the source-frame luminosity in the band corresponding to the 0.3 keV – 10 keV band in the lab frame, i.e. the luminosity observable by *Swift*.

We use GRB 130603B as a representative example of X-ray plateaux following sGRBs because it has a known redshift[36] and has been inferred to spin down under magnetic-dipole braking.[19] We display the observed light curve in Fig. 1 and overplot with a projected light curve from the PWNe model. Black crosses are observations of GRB 130603B by *Swift* and corrected to the source frame. The blue curve is the X-ray light curve predicted by the PWNe model with $B = 10\,{\rm G}$, $B_0 = 4 \times 10^{15}\,{\rm G}$, $\Omega_0/2\pi = 140\,{\rm Hz}$, and $a = 2.8$. The parameters are chosen by hand, guided by results from Ref. 26. The observed and predicted light curve are in broad agreement.

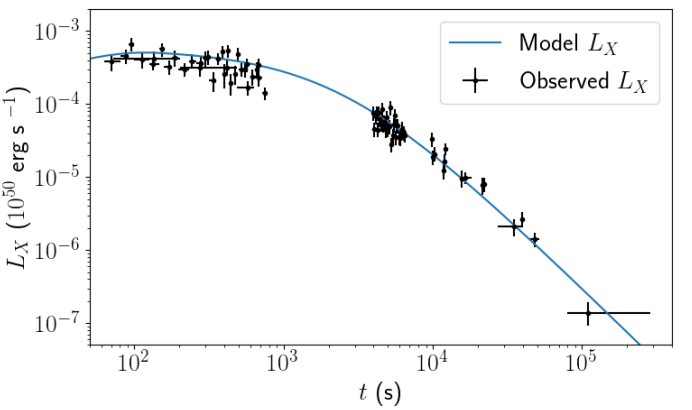

Fig. 1. X-ray luminosity in the source frame $L_{\rm X}\,(10^{50}{\rm erg\,s^{-1}})$ versus time $t\,({\rm s})$. Here "X-ray" refers to the 0.3 keV – 10 keV band observable by *Swift* corrected to the source frame. Black crosses are observations of GRB 130603B by *Swift* and corrected to the source frame. The blue curve is the X-ray light curve predicted by the PWNe model with $B = 10\,{\rm G}$, $B_0 = 4 \times 10^{15}\,{\rm G}$, $\Omega_0/2\pi = 140\,{\rm Hz}$, and $a = 2.8$. Parameters chosen by hand, guided by results from Ref. 26.

In some cases, such as GRB 090515, the plateau ends abruptly. In the context of the central engine model, this has been interpreted as the neutron star collapsing to a black hole and terminating energy injection[18] (we note, however, recent population-based arguments against this hypothesis[37]). In the PWNe model, the collapse of the neutron star halts injection only but does not remove the existing population of electrons, so the afterglow persists for some time, given approximately by the synchrotron lifetime $t_{\rm synch} \sim 2 \times 10^{-9}\,[B/(1\,{\rm G})]^{-3/2}\,[\nu_c/(1\,{\rm keV})]^{-1/2}$ s. In the X-ray band, and for the parameters in Figure 1, $t_{\rm synch}$ amounts to nanoseconds.

3.1. *Luminosity-time correlation*

The Dainotti correlation connects the plateau luminosity $L_{\rm p}$ and plateau duration $t_{\rm p}$ in GRB plateaux which states that brighter plateaux have shorter durations than dimmer plateaux.[3,38,39] This correlation has been studied extensively for LGRBs under a variety of assumptions[40,41] (see Ref. 42 for a thorough review on the correlation and its uses).

The PWNe model presented in Ref. 25 naturally reproduces the observed correlation for reasonable definitions of $L_{\rm p}$ and $t_{\rm p}$. One reasonable choice is to define the X-ray plateau duration as $t_{\rm p} = \tau$ and the corresponding luminosity as $L_{\rm p} = L_{\rm X}(t = \tau)$. The light blue region in Fig. 2 indicates the full range of $(L_{\rm p}, t_{\rm p})$ pairs generated by the PWNe model for $B = 5.0 \times 10^{-1}\,{\rm G}$, $E_{-0} = 2.5 \times 10^{-2}\,{\rm erg}$, $10^{12} \leq B_0/(1\,{\rm G}) \leq 10^{16}$, and $\Omega_0/2\pi \leq 10^3\,{\rm Hz}$. The black line and grey-shaded region corresponds to the best-fit correlation from Ref. 18 based on a sample of 159 sGRBs and LGRBs. The observed correlation falls entirely within the range permitted by the PWNe model.

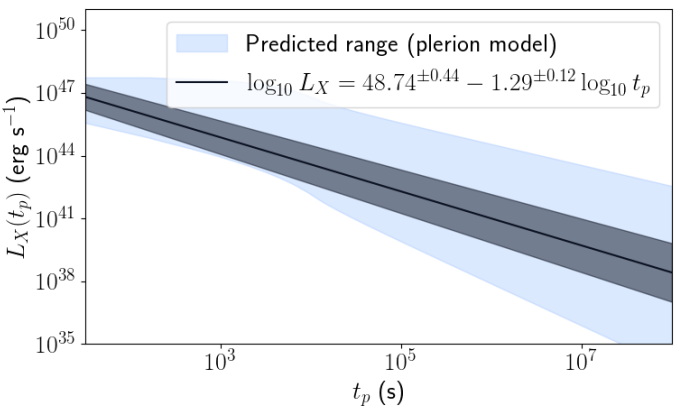

Fig. 2. X-ray plateau luminosity in the source frame $L_{\rm p} = L_{\rm X}(t_{\rm p})\,({\rm erg\,s^{-1}})$ versus X-ray plateau duration $t_{\rm p}$ (s). The black line and grey-shaded region correspond to the best-fit correlation from Ref. 18 from a sample of 159 GRBs. The light blue shaded region corresponds to the range of $(L_{\rm p}, t_{\rm p})$ pairs generated by the PWNe model for $B = 5.0 \times 10^{-1}\,{\rm G}$, $10^{12} \leq B_0/(1\,{\rm G}) \leq 10^{16}$, and $\Omega_0/2\pi \leq 10^3\,{\rm Hz}$. Model parameters were chosen based on results presented in Ref. 26.

4. Inferring Parameters of the Central Engine

In this section, we review results presented in Ref. 26 inferring B_0, Ω_0, $E_{\pm 0}$, a, and (for model B) B using the X-ray afterglow for six sGRBs of known redshift with an X-ray plateau. We reproduce here the necessary physics to interpret the results and leave the details of the analysis to Ref. 26.

The source-frame synchrotron spectrum at time t is

$$F_\nu(t,\nu) = N(E,t)\left.\frac{\mathrm{d}E}{\mathrm{d}t}\right|_{\mathrm{synch}}\frac{\mathrm{d}E}{\mathrm{d}\nu}. \tag{7}$$

The synchrotron cooling rate and the characteristic synchrotron frequency depend on the magnetic field in the bubble, which is determined by B_0 and Ω_0 in model A and by B in model B. The dependence on $N(E,t)$ indicates F_ν is dependent on B, B_0, Ω_0, $E_{\pm0}$, and a, so a single point-in-time spectrum is sufficient to infer posteriors on each parameter. For a full discussion of the results and method, see Sec. 4 in Ref. 26. For both models, one has a neutron star with an approximately millisecond spin period ($\Omega_0/2\pi \lesssim 10^3\,\mathrm{Hz}$) and a magnetar-strength poloidal magnetic field ($B_0 \sim 10^{15}\,\mathrm{G}$) i.e. a millisecond magnetar. The correlations between B_0 and Ω_0 reflect their relation to the spin-down luminosity $L_0 \propto B_0^2\Omega_0^4$ and $\tau \propto B_0^{-2}\Omega_0^{-2}$. For model B, the posteriors on B cover the range $10^{-1} \lesssim B/(1\,\mathrm{G}) \lesssim 1$. This is much stronger than the magnetic field in the interstellar medium ($\sim 10^{-6}\,\mathrm{G}$) but smaller than the expected field advected outwards from the central object by the relativistic outflow (i.e. the magnetic field in model A). For both models, $E_{-0} \sim 10^{-3}\,\mathrm{erg}$, which is consistent with a population of electrons accelerated in the magnetar's magnetosphere and injected into the magnetar wind with a radiation-reaction-limited Lorentz factor.

4.1. *Spectral evolution*

In this section, we review briefly results presented in Ref. 26 using the spectrum of GRB 130603B at four separate epochs to infer B_0, Ω_0, $E_{\pm0}$, a, and B for each epoch. We label each epoch t_i with corresponding magnetic field B_i for $i \in [1,4]$ and use log uniform priors such that $10^{-6} < B_i/(1\,\mathrm{G}) < 10^6$. For each epoch with flux data F_{ν_i}, flux uncertainty σ_i, and model flux $F_\nu(t_i,\nu)$ given by Eq. (7), we define a Gaussian likelihood $P_i \propto \exp\left\{\left[F_{\nu_i} - F_\nu\left(t_i,\nu\right)\right]^2 / \left(2\sigma_i^2\right)\right\}$ such that the priors on B_0, Ω_0, $E_{\pm0}$ and a are the same at each epoch. The analysis is performed on the joint likelihood $\Pi_i P_i$.

The median values of the posterior describe a millisecond magnetar with $B_0 \approx 2\times10^{15}\,\mathrm{G}$ and $\Omega_0/2\pi \approx 600\,\mathrm{Hz}$, supplying the remnant with relativistic electrons with $a \approx 1.9$, $E_{-0} \approx 3.2\times10^{-5}\,\mathrm{erg}$, and $E_{+0} \approx 1\,\mathrm{erg}$. The median magnetic fields B_i suggest the field drops at an average rate of $0.04\,\mathrm{G\,s^{-1}}$ from $B_1 = 2\times10^2\,\mathrm{G}$ at $t_1 = 643\,\mathrm{s}$ to $B_4 = 5\times10^{-1}\,\mathrm{G}$ at $t_4 = 5735\,\mathrm{s}$. This is both slower and weaker than what is expected for the field in the termination shock of the wind in model A, which scales roughly as $B(t) \propto B_0 t^{-2}$ for $t \gtrsim \tau$, if the wind expands at a constant, relativistic speed (as in Ref. 25). The scale and temporal evolution of the B_i indicate the time-dependent magnetic field in the bubble requires revision. Several mechanisms for this are discussed in Ref. 26, including varying the expansion rate of the bubble or choosing an entirely separate magnetic field configuration.

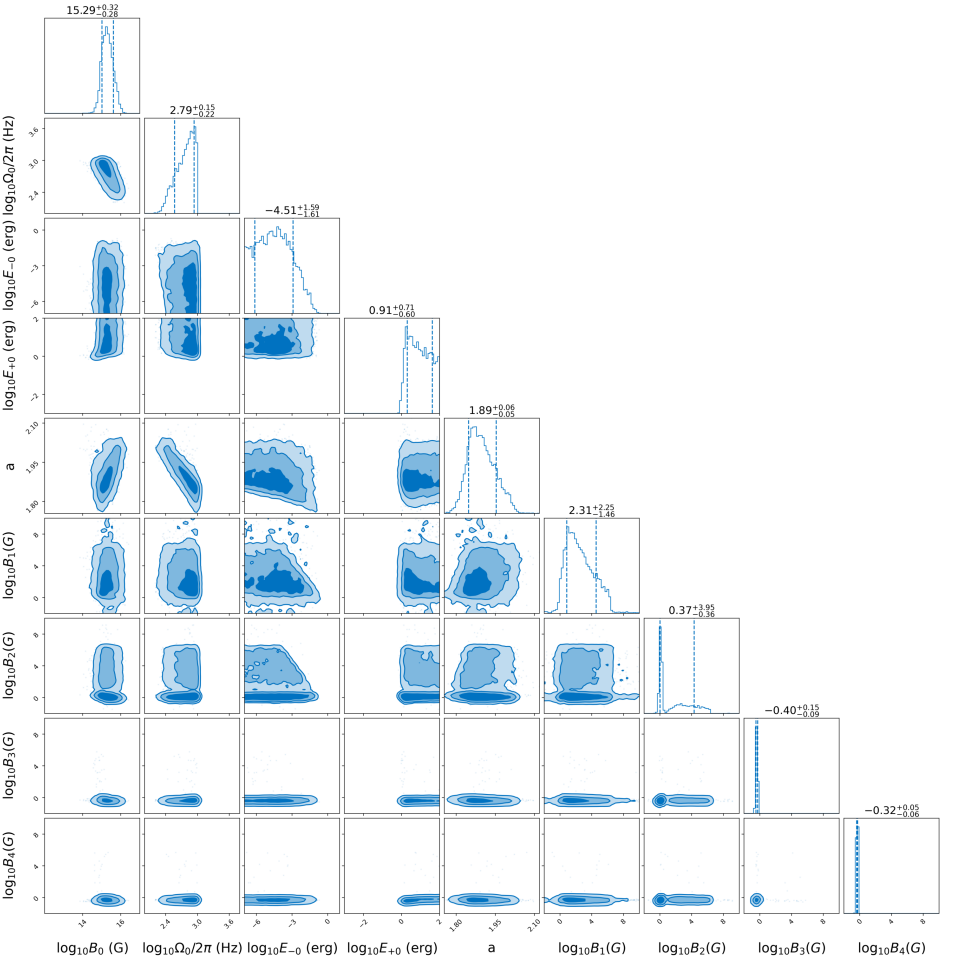

Fig. 3. Corner plot showing the posterior distribution obtained for four instantaneous spectra for GRB130603B for the parameters $\log_{10} B_0$ (G), $\log_{10} \Omega_0/2\pi$ (Hz), $\log_{10} E_{\pm 0}$ (erg), a, and $\log_{10} B_i$ $(1 \leq i \leq 4)$ (G). Figure reproduced from Ref. 26

5. Conclusion

A millisecond magnetar engine based on classic models of PWNe can explain some of the observed features of canonical sGRB afterglows. Plateau light curves are broadly consistent with the synchrotron output of an electron population $N(E, t)$ evolving under ongoing, power-law injection and adiabatic and synchrotron cooling. Such a model may be referred to as a plerion model (as in Ref. 25 and Ref. 26) or, as a synonym, a PWNe model (as we do in this work). The model is able to reproduce both the shape of the afterglow and correlations L_p–t_p. Furthermore, the instantaneous spectra can be used to infer B, B_0, Ω_0, $E_{\pm 0}$, and a within the context of the model. However, the model summarized here (originally in Ref. 25)

is highly idealized and does not include the important effects of merger ejecta on the evolution of the remnant (considered in e.g. Refs. 20–22). Also, as presented in Ref. 26, the temporal evolution of the spectrum implies a magnetic field that is inconsistent with both a dipole field (model A) and a constant field (model B). Future modeling improving on the work in Ref. 25 and integrating it into existing models for sGRB remnants should ultimately be compared to a broad sample of sGRBs.

Acknowledgments

This work makes use of data supplied by the UK Swift Science Data Centre at the University of Leicester. Parts of this research were conducted by the Australian Research Council Centre of Excellence for Gravitational Wave Discovery (OzGrav), through Project Number CE170100004. The work is also supported by an Australian Research Council Discovery Project grant (DP170103625).

References

1. B. Zhang, Y. Z. Fan, J. Dyks, S. Kobayashi, P. Mészáros, D. N. Burrows, J. A. Nousek and N. Gehrels, Physical Processes Shaping Gamma-Ray Burst X-Ray Afterglow Light Curves: Theoretical Implications from the Swift X-Ray Telescope Observations, *ApJ* **642**, 354 (May 2006).
2. J. A. Nousek, C. Kouveliotou, D. Grupe, K. L. Page, J. Granot, E. Ramirez-Ruiz, S. K. Patel, D. N. Burrows, V. Mangano, S. Barthelmy, A. P. Beardmore, S. Campana, M. Capalbi, G. Chincarini, G. Cusumano, A. D. Falcone, N. Gehrels, P. Giommi, M. R. Goad, O. Godet, C. P. Hurkett, J. A. Kennea, A. Moretti, P. T. O'Brien, J. P. Osborne, P. Romano, G. Tagliaferri and A. A. Wells, Evidence for a Canonical Gamma-Ray Burst Afterglow Light Curve in the Swift XRT Data, *ApJ* **642**, 389 (May 2006).
3. M. G. Dainotti, V. F. Cardone and S. Capozziello, A time-luminosity correlation for γ-ray bursts in the X-rays, *Monthly Notices of the Royal Astronomical Society* **391**, L79 (November 2008).
4. M. G. Dainotti, R. Willingale, S. Capozziello, V. Fabrizio Cardone and M. Ostrowski, Discovery of a Tight Correlation for Gamma-ray Burst Afterglows with "Canonical" Light Curves, *ApJL* **722**, L215 (October 2010).
5. A. Rowlinson, B. P. Gompertz, M. Dainotti, P. T. O'Brien, R. A. M. J. Wijers and A. J. van der Horst, Constraining properties of GRB magnetar central engines using the observed plateau luminosity and duration correlation, *Monthly Notices of the Royal Astronomical Society* **443**, 1779 (September 2014).
6. N. Rea, M. Gullón, J. A. Pons, R. Perna, M. G. Dainotti, J. A. Miralles and D. F. Torres, Constraining the grb-magnetar model by means of the galactic pulsar population, *The Astrophysical Journal* **813**, p. 92 (2015).
7. B. P. Abbott *et al.*, GW170817: Observation of Gravitational Waves from a Binary Neutron Star Inspiral, *Physical Review Letters* **119**, p. 161101 (2017).
8. B. P. Abbott *et al.*, Gravitational Waves and Gamma-Rays from a Binary Neutron Star Merger: GW170817 and GRB 170817A, *The Astrophysical Journal Letters* **848** (2017).

9. M. J. Rees and P. Mészáros, Refreshed Shocks and Afterglow Longevity in Gamma-Ray Bursts, *ApJL* **496**, L1 (March 1998).
10. M. G. Dainotti, A. Ł. Lenart, N. Fraija, S. Nagataki, D. C. Warren, B. De Simone, G. Srinivasaragavan and A. Mata, Closure relations during the plateau emission of Swift GRBs and the fundamental plane, *Publications of the Astronomical Society of Japan* **73**, 970 (August 2021).
11. T. Piran, Gamma-ray bursts and the fireball model, *Physics Reports* **314**, 575 (June 1999).
12. P. Kumar, R. Narayan and J. L. Johnson, Properties of Gamma-Ray Burst Progenitor Stars, *Science* **321**, p. 376 (July 2008).
13. Z. G. Dai and T. Lu, Gamma-ray burst afterglows and evolution of postburst fireballs with energy injection from strongly magnetic millisecond pulsars, *Astronomy and Astrophysics* **333**, L87 (May 1998).
14. B. Zhang and P. Mészáros, Gamma-Ray Burst Afterglow with Continuous Energy Injection: Signature of a Highly Magnetized Millisecond Pulsar, *The Astrophysical Journal* **552**, L35 (May 2001).
15. B. Zhang and P. Mészáros, Gamma-Ray Burst Afterglow with Continuous Energy Injection: Signature of a Highly Magnetized Millisecond Pulsar, *ApJ Letters* **552**, L35 (May 2001).
16. Y. Fan and D. Wei, Late internal-shock model for bright x-ray flares in gamma-ray burst afterglows and grb 011121, *Monthly Notices of the Royal Astronomical Society: Letters* **364**, L42 (2005).
17. B. P. Gompertz, P. T. O'Brien, G. A. Wynn and A. Rowlinson, Can magnetar spin-down power extended emission in some short GRBs?, *Monthly Notices of the Royal Astronomical Society* **431**, 1745 (May 2013).
18. A. Rowlinson, P. T. O'Brien, B. D. Metzger, N. R. Tanvir and A. J. Levan, Signatures of magnetar central engines in short GRB light curves, *Monthly Notices of the Royal Astronomical Society* **430**, 1061 (April 2013).
19. P. D. Lasky, C. Leris, A. Rowlinson and K. Glampedakis, The braking index of millisecond magnetars, *The Astrophysical Journal Letters* **843**, p. L1 (2017).
20. B. D. Metzger and A. L. Piro, Optical and X-ray emission from stable millisecond magnetars formed from the merger of binary neutron stars, *Montly Notices of the Royal Astronomical Society* **439**, 3916 (April 2014).
21. D. M. Siegel and R. Ciolfi, Electromagnetic Emission from Long-lived Binary Neutron Star Merger Remnants. I. Formulation of the Problem, *ApJ* **819**, p. 14 (March 2016).
22. Y.-W. Yu, B. Zhang and H. Gao, Bright "Merger-nova" from the Remnant of a Neutron Star Binary Merger: A Signature of a Newly Born, Massive, Millisecond Magnetar, *ApJL* **776**, p. L40 (October 2013).
23. G. Stratta, M. G. Dainotti, S. Dall'Osso, X. Hernandez and G. De Cesare, On the Magnetar Origin of the GRBs Presenting X-Ray Afterglow Plateaus, *ApJ* **869**, p. 155 (December 2018).
24. N. Sarin, P. D. Lasky and G. Ashton, Interpreting the X-ray afterglows of gamma-ray bursts with radiative losses and millisecond magnetars, *Monthly Notices of the Royal Astronomical Society* **499**, 5986 (December 2020).
25. L. C. Strang and A. Melatos, Plerion model of the X-ray plateau in short gamma-ray bursts, *arXiv e-prints*, p. arXiv:1906.02877 (June 2019).
26. L. C. Strang, A. Melatos, N. Sarin and P. D. Lasky, Inferring properties of neutron stars born in short gamma-ray bursts with a plerion-like X-ray plateau, *Monthly Notices of the Royal Astronomical Society* **507**, 2843 (October 2021).

27. F. Pacini and M. Salvati, On the Evolution of Supernova Remnants. Evolution of the Magnetic Field, Particles, Content, and Luminosity, *The Astrophysical Journal* **186**, 249 (November 1973).
28. M. J. Rees and J. E. Gunn, The origin of the magnetic field and relativistic particles in the Crab Nebula, *Monthly Notices of the Royal Astronomical Society* **167**, 1 (April 1974).
29. R. D. Blandford and C. F. McKee, Fluid dynamics of relativistic blast waves, *Physics of Fluids* **19**, 1130 (August 1976).
30. C. F. Kennel and F. V. Coroniti, Confinement of the Crab pulsar's wind by its supernova remnant, *The Astrophysical Journal* **283**, 694 (August 1984).
31. A. Melatos and D. B. Melrose, Energy transport in a rotation-modulated pulsar wind, *Monthly Notices of the Royal Astronomical Society* **279**, 1168 (April 1996).
32. S. V. Bogovalov, D. V. Khangulyan, A. V. Koldoba, G. V. Ustyugova and F. A. Aharonian, Modelling interaction of relativistic and non-relativistic winds in binary system PSR B1259-63/SS2883 - I. Hydrodynamical limit, *Monthly Notices of the Royal Astronomical Society* **387**, 63 (June 2008).
33. N. Gehrels, G. Chincarini, P. Giommi, K. O. Mason, J. A. Nousek, A. A. Wells, N. E. White, S. D. Barthelmy, D. N. Burrows, L. R. Cominsky, K. C. Hurley, F. E. Marshall, P. Mészáros, P. W. A. Roming, L. Angelini, L. M. Barbier, T. Belloni, S. Campana, P. A. Caraveo, M. M. Chester, O. Citterio, T. L. Cline, M. S. Cropper, J. R. Cummings, A. J. Dean, E. D. Feigelson, E. E. Fenimore, D. A. Frail, A. S. Fruchter, G. P. Garmire, K. Gendreau, G. Ghisellini, J. Greiner, J. E. Hill, S. D. Hunsberger, H. A. Krimm, S. R. Kulkarni, P. Kumar, F. Lebrun, N. M. Lloyd-Ronning, C. B. Markwardt, B. J. Mattson, R. F. Mushotzky, J. P. Norris, J. Osborne, B. Paczynski, D. M. Palmer, H. S. Park, A. M. Parsons, J. Paul, M. J. Rees, C. S. Reynolds, J. E. Rhoads, T. P. Sasseen, B. E. Schaefer, A. T. Short, A. P. Smale, I. A. Smith, L. Stella, G. Tagliaferri, T. Takahashi, M. Tashiro, L. K. Townsley, J. Tueller, M. J. L. Turner, M. Vietri, W. Voges, M. J. Ward, R. Willingale, F. M. Zerbi and W. W. Zhang, The Swift Gamma-Ray Burst Mission, *The Astrophysical Journal* **611**, 1005 (August 2004).
34. P. A. Evans, A. P. Beardmore, K. L. Page, L. G. Tyler, J. P. Osborne, M. R. Goad, P. T. O'Brien, L. Vetere, J. Racusin, D. Morris, D. N. Burrows, M. Capalbi, M. Perri, N. Gehrels and P. Romano, An online repository of Swift/XRT light curves of γ-ray bursts, *Astronomy and Astrophysics* **469**, 379 (July 2007).
35. P. A. Evans, A. P. Beardmore, K. L. Page, J. P. Osborne, P. T. O'Brien, R. Willingale, R. L. C. Starling, D. N. Burrows, O. Godet, L. Vetere, J. Racusin, M. R. Goad, K. Wiersema, L. Angelini, M. Capalbi, G. Chincarini, N. Gehrels, J. A. Kennea, R. Margutti, D. C. Morris, C. J. Mountford, C. Pagani, M. Perri, P. Romano and N. Tanvir, Methods and results of an automatic analysis of a complete sample of Swift-XRT observations of GRBs, *Monthly Notices of the Royal Astronomical Society* **397**, 1177 (August 2009).
36. A. Melandri, M. de Pasquale, S. D. Barthelmy, D. N. Burrows, M. H. Siegel and N. Gehrels, Swift Observation of GRB130603B, *GCN Report* **442** (2013).
37. P. Beniamini and W. Lu, Survival times of supramassive neutron stars resulting from binary neutron star mergers, *arXiv e-prints*, p. arXiv:2104.01181 (April 2021).
38. M. G. Dainotti, R. Willingale, S. Capozziello, V. Fabrizio Cardone and M. Ostrowski, Discovery of a Tight Correlation for Gamma-ray Burst Afterglows with "Canonical" Light Curves, *The Astrophysical Journal* **722**, L215 (October 2010).
39. J. Sultana, D. Kazanas and K. Fukumura, Luminosity Correlations for Gamma-Ray Bursts and Implications for Their Prompt and Afterglow Emission Mechanisms, *The Astrophysical Journal* **758**, p. 32 (October 2012).

40. M. G. Dainotti, S. Postnikov, X. Hernandez and M. Ostrowski, A Fundamental Plane for Long Gamma-Ray Bursts with X-Ray Plateaus, *The Astrophysical Journal* **825**, p. L20 (July 2016).
41. M. G. Dainotti, A. D. Boria and J. F. Arratia, Gamma-ray bursts with afterglow plateau phases associated with supernovae, in *Fourteenth Marcel Grossmann Meeting - MG14*, eds. M. Bianchi, R. T. Jansen and R. Ruffini, January 2018.
42. M. Dainotti, *Gamma-ray Burst Correlations; Current status and open questions* 2019.